Assessment of Landslide risk using BLR and AHP for South Sikkim Himalaya, India

Sarkar Kallol[1*] and Mandal Sujit[2]
1. Department of Geography, University of Gour Banga, 732103, INDIA
2. Department of Geography, Diamond Harbour Women's University, West Bengal, 743368, INDIA
*kallol.kallolsarkar@gmail.com

Abstract
South Sikkim Himalaya i.e. south district of Sikkim is a very landslide prone area. The present study dealt with the preparation of landslide susceptibility zonation map, risk exposures map and landslide risk zonation map of South Sikkim Himalaya. First, fourteen landslide causative factors have been considered and corresponding thematic data layers have also been extracted in Arc GIS (10.1) and Geomatica (2016) software environments to prepare landslide susceptibility map using binary logistic regression (BLR) model. The landslide susceptibility map has been grouped into four such as sever, high, medium and low. Five landslide vulnerability components such as land use/land cover, population density, number of household, building typology and height were considered to develop risk exposure maps. Then landslide susceptibility map and all risk exposure maps were being combined using analytical hierarchy process (AHP) to generate socio-economic risk and structural risk map of South Sikkim Himalaya. Both risk maps were classified into four i.e. severe, high, medium and low.

In South Sikkim Himalaya about 40% area falls under the high risk zone. Namchi, Mamring, Melli, Jorethang, Manpur and Yangyang are in severe risk zone. Both the socio-economic and structural risk maps will expect to play important roles in landslide impose disaster mitigation and management of the South Sikkim Himalaya. The study depicted that human infrastructures are closely associated with both risks.

Keywords: Landslide vulnerability and risk, binary logistic regression (BLR), analytical hierarchy process (AHP), geo-spatial technology, South Sikkim Himalaya.

Introduction

The requirement of evaluation of landslide risk of existing built-up areas in terms of damage potential of its urban and rural structures and socio-economic set-up when impacted by a lethal landslide has become an important issue in the Indian context. The number of sufferers in a landslide is related to the susceptibility of local houses, population density and the destruction power of landslide. Manmade structures are always affected by landslide.

***** Author for Correspondence***

There is a chance of partial damage to complete destruction of residential houses on unstable slopes as landslides destabilize or destroy foundation. Landslides also destroy utilities such as water pipelines, communication lines, power lines and transport routes. If commercial structures face destruction like residential buildings, the local economy could be negatively affected because landslides disrupt transport systems which create shut down in trade and commerce.

All the man made facilities like residential, commercial and industrial buildings, educational institutes, hospitals, transportation systems, bridges, pipelines, power plants andcommunication systems are vulnerability exposure. For the safety and sustainability of urban and rural regions, it is necessary to execute long range planning and risk estimation tools that depend on an accurate and multidisciplinary urban and rural modelling. Various researchers around the world have analyzed landslide vulnerability and risk through remote sensing and GIS techniques[1,2]. Different researchers have prepared landslide susceptibility zonation map by using different model to understand landslide risk in RS and GIS environment[3-12]. Some researchers analysed landslide hazard through current techniques and they also discussed relationship between landslide risk evaluation and sustainable development[13-15].

Jibson et al[16] used specific model to prepare digital probabilistic seismic hazard maps. Ghosh et al[17] prepared event based landslide inventory maps to estimate landslide risk. Atkinson and Massari[18] used generalized linear model for construction of landslide susceptibility zonation map to evaluate landslide vulnerability. Gokceoglu et al[19] applied probabilistic model for landslide risk evaluation. Various researchers used logistic regression model to prepare landslide susceptibility zonation to determine which areas are most affected by slope failure[20-24].

Analytical Hierarchy Process (AHP) is also a very effective and popular method for estimation of landslide susceptibility in regional level[25-29]. Except estimation of landslide susceptibility zonation, AHP method is also used in different fields. Murmu et al[30] used AHP method to delineate groundwater potential zones in Dumka district, Jharkhand, India.

According to demand, several researchers in India studied landslides in different mountainous and hilly tracts of the country. They analysed landslide hazard on the basis of landslide causative and triggering factors, landslide susceptibility and risk assessment and mitigation measures.

From their assessment significant information regarding hill slope instability and landslide risk have been achieved[31-37].

South Sikkim Himalaya i.e. south district of Sikkim is the second largest populated district. Though this area is smaller in size but it is thickly populated. Due to population growth and development of tourism industry, new buildings and roads are being constructed, making this hill area increasingly vulnerable day by day[38]. Intense rainfall, earthquakes, steep slopes and ruggedness are the major factors which make this area more vulnerable to landslide disasters.

Objectives of the study

South Sikkim Himalaya is a landslide prone area; especially along the different road corridors, frequent landslides occurred. As a result, not only the transport and communication system was disrupted, but also the economic system in the entire South district of Sikkim was damaged, people lost their lives, hence, the overall development of the entire district came to a standstill. The main aim of this study is to identify the vulnerability and risk of landslide in South Sikkim Himalaya in order to solve the above mentioned problems and to analyze the impact of landslides on human life.

The Study area

The study area lies between 27°4'44" N to 27°31'49"N and 88°15'5" E to 88°32'14"E (Fig. 1). The total geographical area of the South Sikkim is 750 sq. Km. The South Sikkim Himalaya has been classified into 14 sub- watersheds for slope instability analysis on the basis of morphometry and land use parameters. The South Sikkim Himalaya is mountainous with various ridges and ravines and it is a part of eastern Himalayas. The altitude of this study area range from 165 to 5677 m above mean sea level. The geological formation of the study area consists of Quaternary deposits of alluvium.

The existence of Gondwana rocks is seen around Namchi. The rock types are shale, sandstone, quartzite and coal. Buxa formation is younger among the Daling group and this formation consists of quartzites, slates and phyllites which are variegated in red and green colour. The soils are formed from the parent rocks of sandstone, phyllite, schist, gneiss and colluvial material. Soil pH level of this area varies between 5 and 6 which indicates acidic to very acidic in reaction. The major soil types of South Sikkim Himalaya are mountain meadow, brown-red and yellow soil and lateritic soil. The mean annual rainfall of South Sikkim Himalaya is 3496 mm.

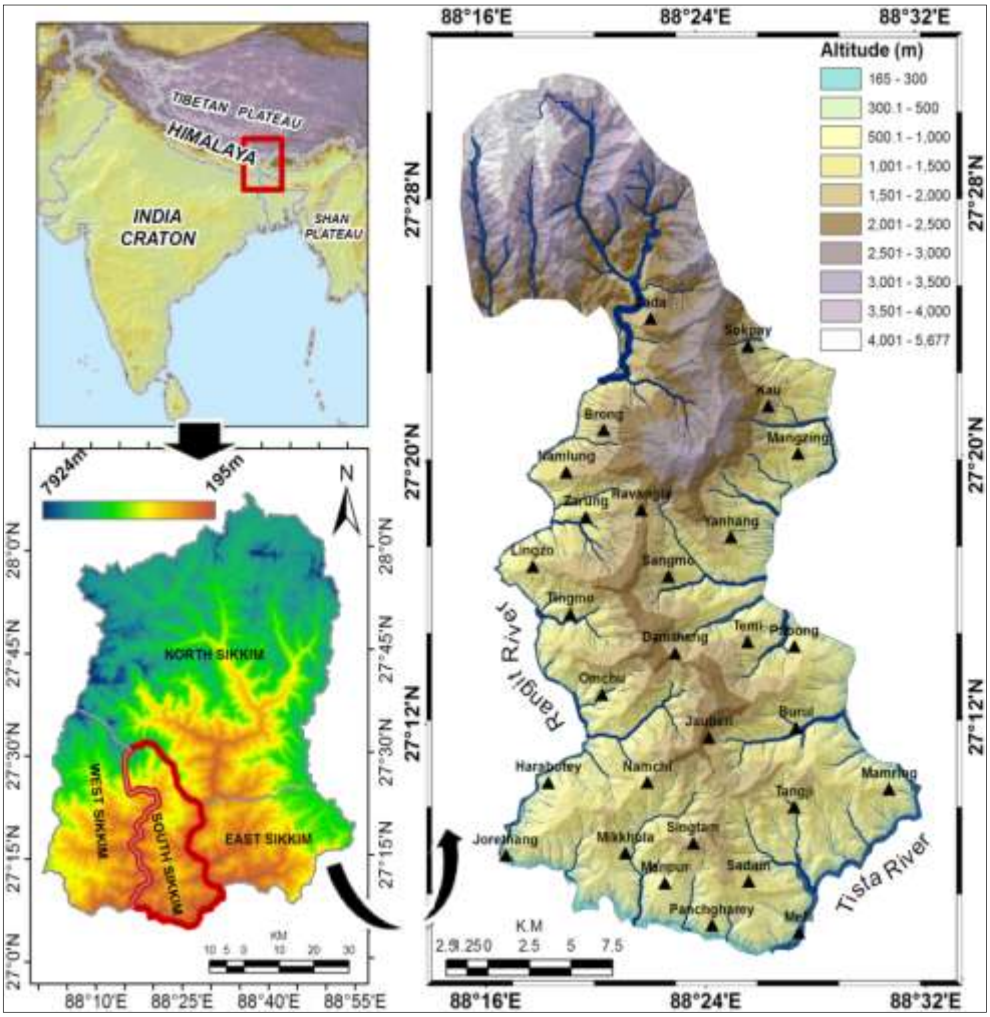

Fig. 1: Location of South Sikkim Himalaya

Data Base and Methodology

Data for making landslide susceptibility map: In order to evaluate landslide susceptibility, the factors affecting landslides have been identified and analysed. On basis of the literature and field investigation, 14 causative/triggering factors i.e. slope, elevation, aspect, drainage, density, distance to drainage, geology, geomorphology, distance to road, road density, distance to lineament, earthquake proximity, lineament density, land use/land cover andrainfall have been taken into account to develop landslide susceptibility zonation map of South Sikkim Himalaya. The thematic layers that have been considered in the present study along with their sources are listed in table 1.

Slope angle, aspect and elevation maps have been prepared from DEM (Fig. 2 a, b and c respectively). Geology and lineament map (Fig. 2 d and j respectively) of the area have extracted from Seismotectonic Atlas of India[39] and Geology map of Sikkim, prepared by GSI, 2007.Geomorphology map (Fig. 2 e) has been collected from G.S.I, NRSC. Land use/ Land cover has been prepared from SENTINEL-2A data (Fig. 2 m) for the year 2018. Maximum likelihood method (MLM) has been applied to classify the digital image Rainfall map (Fig. 2 n) prepared from http://www. worldclim.org data. Each thematic factor has been sub-divided into different classes based on its value or feature.

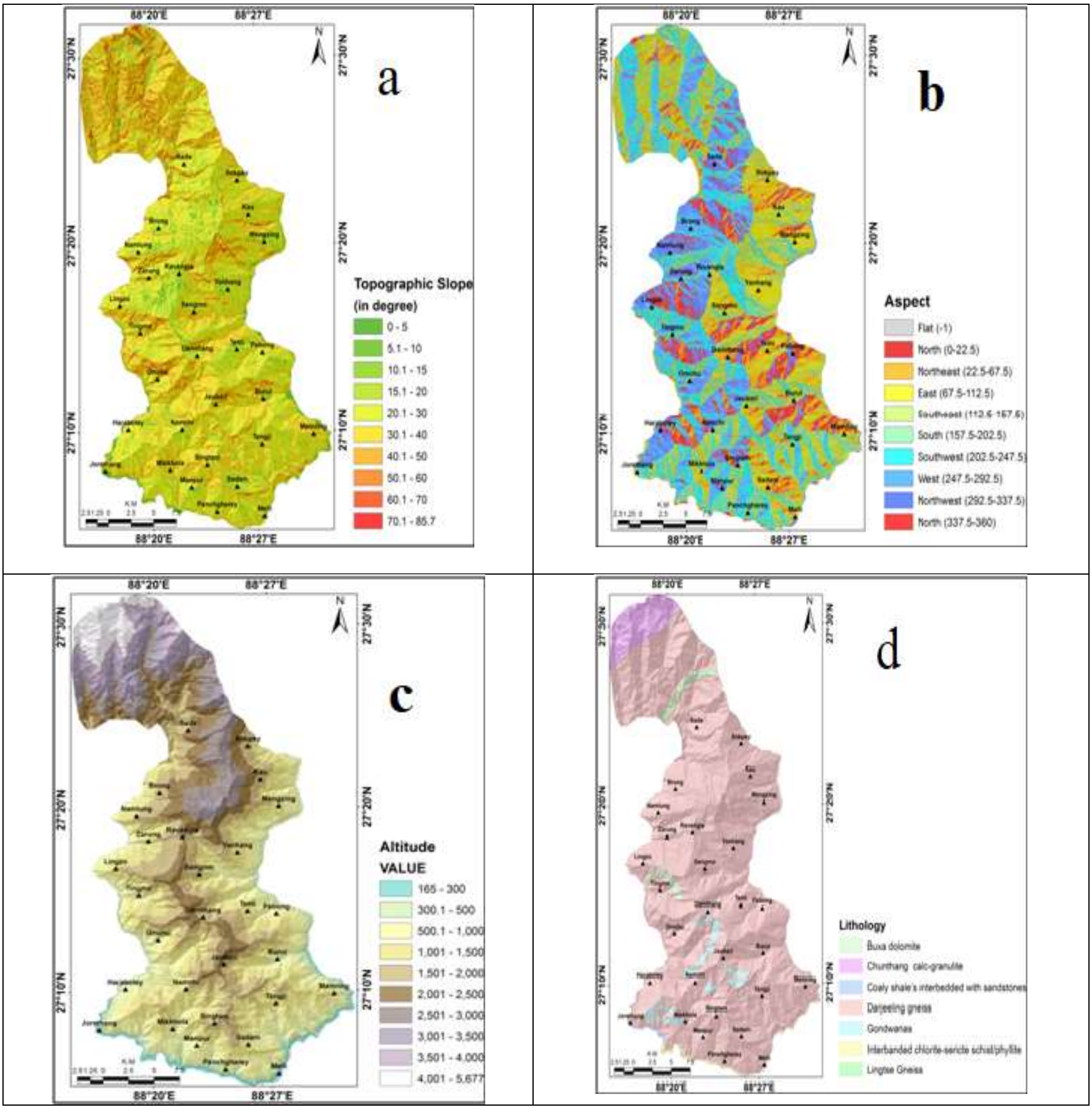

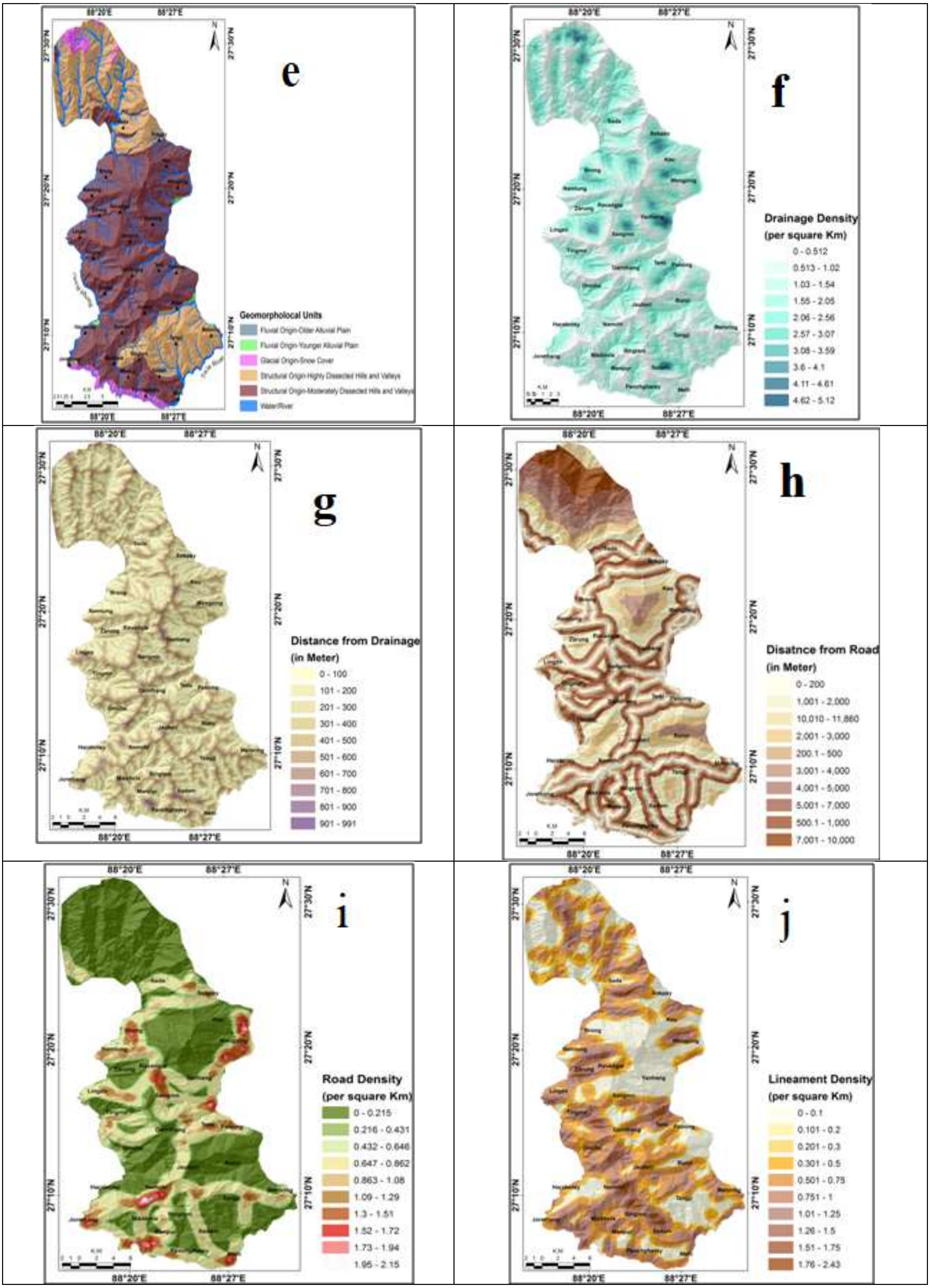
e
Geomorpholocal Units
Fluvial Origin-Older Alluvial Plain
Fluvial Origin-Younger Alluvial Plain
Glacial Origin-Snow Cover
Structural Origin-Highly Dissected Hills and Valleys
Structural Origin-Moderately Dissected Hills and Valleys
Water/River
f
Drainage Density
(per square Km)
0 - 0.512
0.513 - 1.02
1.03 - 1.54
1.55 - 2.05
2.06 - 2.56
2.57 - 3.07
3.08 - 3.59
3.6 - 4.1
4.11 - 4.61
4.62 - 5.12
g
Distance from Drainage
(in Meter)
0 - 100
101 - 200
201 - 300
301 - 400
401 - 500
501 - 600
601 - 700
701 - 800
801 - 900
901 - 991
h
Disatnce from Road
(in Meter)
0 - 200
1,001 - 2,000
10,010 - 11,860
2,001 - 3,000
200.1 - 500
3,001 - 4,000
4,001 - 5,000
5,001 - 7,000
500.1 - 1,000
7,001 - 10,000
i
Road Density
(per square Km)
0 - 0.215
0.216 - 0.431
0.432 - 0.646
0.647 - 0.862
0.863 - 1.08
1.09 - 1.29
1.3 - 1.51
1.52 - 1.72
1.73 - 1.94
1.95 - 2.15
j
Lineament Density
(per square Km)
0 - 0.1
0.101 - 0.2
0.201 - 0.3
0.301 - 0.5
0.501 - 0.75
0.751 - 1
1.01 - 1.25
1.26 - 1.5
1.51 - 1.75
1.76 - 2.43
88°20'E
88°27'E
27°30'N
27°20'N
27°10'N

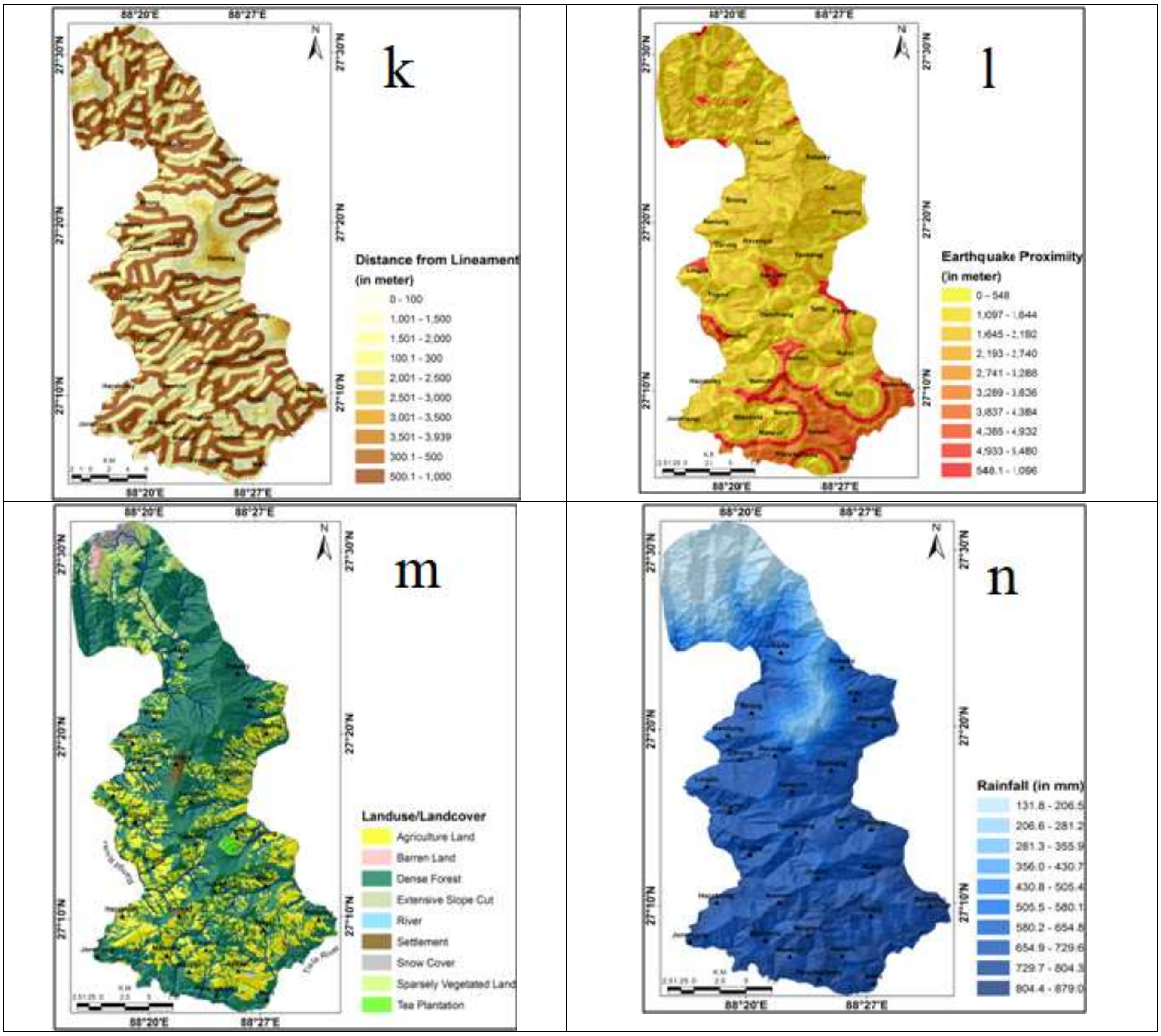

Fig. 2: Thematic data layers; a Slope, b Aspect, c Elevation, d Lithology, e geomorphology, f Drainage density, g Distance to drainage, h Distance to road, Road density, j Lineament density, k Distance to lineament Earthquake proximity, m land use/land cover, n Rainfall

All the thematic data layers have been converted from vector to raster to make raster data layers of South Sikkim Himalaya with 12.5x12.5 m pixels. The total number of pixels containing landslide is 346 out of 471028.

On the basis of Google Earth image interpretation, the landslide inventory map (Fig.3) has been prepared and the map has also been cross-checked by multiple field survey. All the prepared thematic data layers have been processed using binary logistic regression model to prepare landslide susceptibility zonation map of South Sikkim Himalaya.

Spatial and Non-Spatial Data for landslide vulnerability exposures: To understand the landslide vulnerability of South Sikkim Himalaya, spatial and non-spatial databases have been used in the present study. Spatial database are building typology, building height, building density, land use/land cover and non- spatial database, population density, household distributions. Unplanned urbanization and construction of houses in unstable slope area are continuously increasing the landslide vulnerability in South Sikkim Himalaya.

Therefore, assessment of landslide vulnerability by recognizing all the factors contributing to landslide risk in terms of socio-economic and structural aspects is very much significant.

Figure 4 illustrates a framework for landslide vulnerability and risk assessment methodology of South Sikkim Himalaya. An accuracy assessment has been done based on the classified and reference data. Computing an error matrix is the most common way to represent the confidence level in the assessment of remote sensing data[40].

Table 1
Database for making landslide susceptibility map

Data	Sources	Sensor	Time/Period	Purpose
DEM	https://earthexplorer.usgs.gov/	Alaska satellite Facility ‘‘ALOS PALSAR DEM’’	2016-08-25	DEM has been used for the development of elevation, slope and aspect thematic attributes
Drainage Network	DEM		2016	Drainage Network has been used for development of distance from stream and Drainage Density thematic attributes.
Land Use and Land Cover.	SENTINEL-2A data has been used for LULC mapping whereas, maximum likelihood method (MLM) has been applied for classify the digital image.	SENTINEL-2A	2018-01-10 Tile Number: T45RXL.	Landuse and Land Cover mapping.
Road	Earth, Google Map, Open Street Map.		2017	Road Network has been used for development of distance from road and Road Density thematic attributes.
Rainfall	http://www.worldclim.org		1950-2010	Spatial distribution of rainfall.
Fault/Lineament	Seismotectonic Atlas of India (Dasgupta et al. 2000); http://bhuvan.nrsc.gov.in/gis/thematic/index.php		2012	Tectonic feature has been used for development of distance from Lineament and Lineament Density thematic attributes.
Earthquake Proximity	Adhikari and Nath (2016)		1900-2016	Seismicity distribution has been used to developed earthquake proximity thematic attribute.
Geology	Seismotectonic Atlas of India (Dasgupta et al.2000); Geology map of Sikkim (GSI,2007)		2007	Surface geological attribution.
Geomorphology	GSI, NRSC; http:// bhuvan.nrsc.gov.in/gis/thematic/index.php		2005-2006	Geomorphological attributes of south Sikkim.

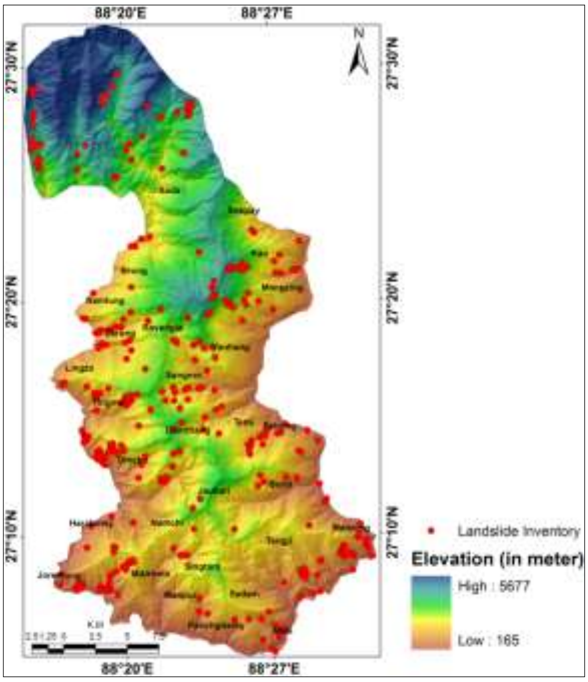

Fig. 3: Landslide inventory map of South Sikkim Himalaya

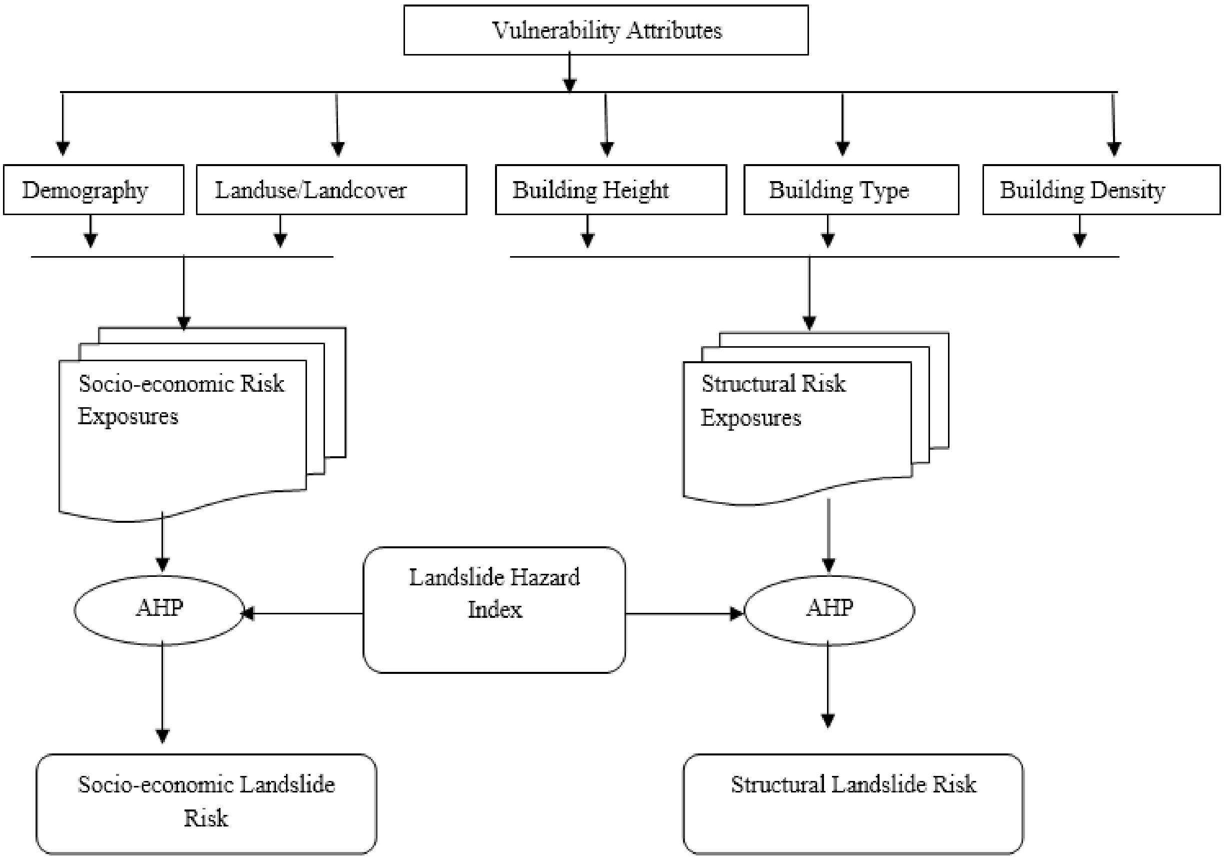

Fig. 4: Landslide vulnerability assessment framework

Error matrices for both socio-economic and structural vulnerability exposures have been prepared for comparisons. Such matrices have been prepared on the basis of accuracy assessment technique of statistical correlations between reference (prepared from Rapid Visual Screening) map data and classified (remote sensing data) data[41,42].

Overall accuracy, user's accuracy, producer's accuracy and kappa value have been used in this study as correlation indicators. The percentage of matched data between the reference and the classified maps is known as an overall accuracy, while user's accuracy denotes the percentage of matched data in the classified map. Producer's accuracy represents the percentage of matched data in the reference map. Kappa value determines the differences between the reference and the chance conformity between both the maps. The kappa value depicts as:

$$k = \frac{N\sum_{i=1}^{r} X_{ii} - \sum_{i=1}^{r}(X_{i+}X_{+i})}{N^2 - \sum_{i=1}^{r}(X_{i+}X_{+i})} \tag{1}$$

where N is the total number of sites in the matrix, r is the number of rows in the matrix, X_{ii} is the number in row i and column i, X_{i+} is the total for row i and X_{+i} is the total for column i[42,43]. The kappa statistics >0.80 proposed strong conformity whereas 0.60 to 0.80 recommended good conformity and when the kappa value is close to 0, it indicates poor conformity[44].

For the accuracy assessment of the vulnerability exposures of this study, two types of data have been taken. Building typology, landuse/ landcover have been derived from satellite imagery and building height map has been generated from Google Earth 3-D aspect, which has been used as classified data. Above mentioned vulnerability exposures were again derived through Rapid Visual Screening from 200 survey locations which have been considered as reference data. In the Rapid Visual Screening process, a hand held GPS has been used for coordinate generation at each of the 200 locations.

Binary Logistic Regression Model and Landslide susceptibility: In this study to generate landslide susceptibility map of South Sikkim Himalaya, Binary Logistic Regression Model has been successfully used. In present study, the dependent variable is landslide and it is a binary variable indicating the presence or absence of landslides. Quantitatively the association between the incident of landslide and several causative factors is revealed using equation:

$$p = \frac{1}{1+e^{-z}} \tag{2}$$

where p denotes predicted probability of landslide incidence based on the impact of causative factors. The probability ranges from 0 to 1 on an S shaped curve[45], whereas z is the linear regression model (Eq. 3) which varies from -∞ to+∞.

$$Z = b_0 + b_1 x_1 + b_2 x_2 + ... + b_n x_n \tag{3}$$

where b_0 is the intercept of linear combination, n is the number of independent variables, $b_1, b_2 ... b_n$ are the coefficients and $x_1, x_2 ..... x_n$ are the causative factors of landslide. Probability (p) of landslide vulnerability ranges from 0 to 1. It indicates high vulnerability when probability is close to value 1 and low vulnerability when it is close to 0. In this study all calculations of logistic regression have been done through SPSS software.

Landslide vulnerability exposures

Population Density: With the help of census data population, vulnerability exposure has been estimated. According to Indian census report (2011), 148 villages and two urban centers (Namchi and Jorethang) are in South district of Sikkim i.e. South Sikkim Himalaya. Population density of 148 villages and two urban centers has been taken to estimate population vulnerability exposure[46] shown in table 2.

The population of South Sikkim Himalaya (South district of Sikkim) increased from 131525 in 2001 to 146850 in 2011. There was change of 11.65 percent in the population compared to population as per 2001. In the previous census of India 2001, South Sikkim Himalaya (South district of Sikkim) recorded increase of 33.39 percent to its population compared to 1991. High population density, age specific population below 7 years and above 65 years, female population, day and night time population are more vulnerable to landslide risk. High population density is observed in Jorethang, Namchi, Yangyang, Mangzing, Temi and Kau areas in South Sikkim Himalaya (Fig. 5).

Household Distribution: Household distributions have been taken into account as a demographic vulnerability exposure. Demographic vulnerability exposure has been estimated based on household distributions in South Sikkim Himalaya[47]. Table 3 shows household distributions of South Sikkim Himalaya. It is observed that household distributions are very high in Namchi and Jorethang area (Fig. 6).

Landuse/landcover (LULC): LULC provides information about predominant land cover and socio-economic attributes of a particular area. In the present study SENTINEL-2A data has been used for LULC mapping whereas maximum likelihood method (MLM) has been applied for classifying the digital image. LULC map of South Sikkim Himalaya is described in fig. 7.

The whole investigation region has been categorized into nine significant LULC units such as agriculture land, barren land, dense forest, extensive slope cut, river, settlement, snow cover, sparsely vegetated land and tea plantation. The accuracy assessment between the 'reference' (RVS derived) and 'classified' (SENTINEL-2A derived) maps has been discussed in table 4.

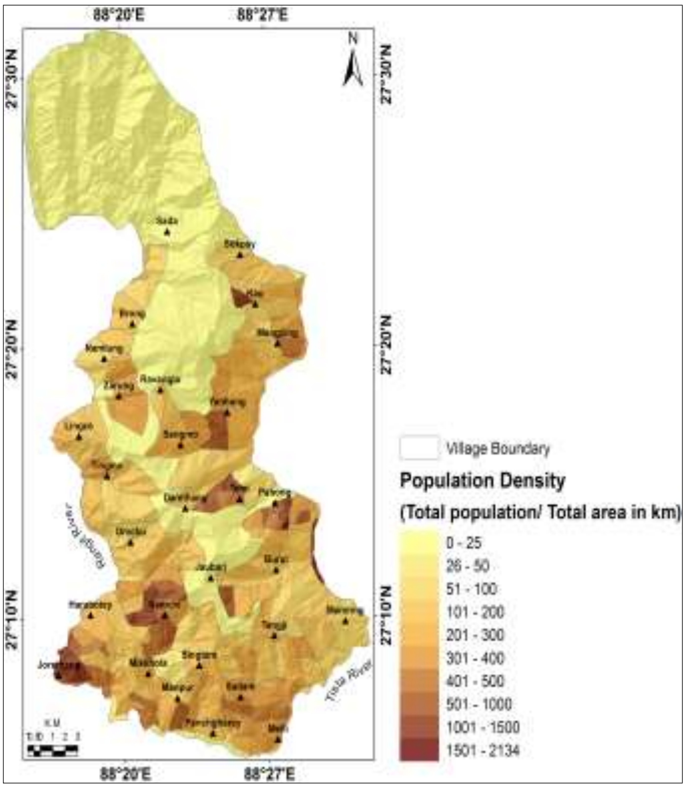

Fig. 5: Population density map

Table 2
Population density of South Sikkim Himalaya (Indian census report 2011)[46]

S. N.	Name of village	Population Density	S.N.	Name of village	Population Density	S.N.	Name of Village	Population Density
1	Omchu	75	51	Sukrabarey	500	101	Brong	139
2	Chumlok	355	52	Sadam	251	102	Poley	232
3	Wak	226	53	Rabitar	254	103	Namlung	147
4	Chemchey	238	54	Rabikhola	220	104	Lingdong	128
5	Damthang	207	55	Tangji	233	105	Ralong	164
6	Jaubari	151	56	Bikmat	241	106	Ralong Moastery	300
7	Tingrithang	203	57	Rateypani	377	107	Deythang	366
8	Mamley	249	58	Passi	164	108	Zarung	246
9	Pabong	147	59	Kateng-Bokrang	189	109	Barfung	965
10	Pajer	161	60	Paleytam	310	110	Bakkhim	339
11	Kamrang	293	61	Nalam-Kolbong	804	111	Kewzing	179
12	Tinzer	166	62	Nagi	232	112	Dalep	337
13	Denchung	246	63	Maneydara	343	113	Lingzo	310
14	poklok	430	64	Kabrey	410	114	Likship	793
15	Tinik	559	65	Karek	357	115	Hingdam	189
16	Chisopani	980	66	Phong	200	116	Lamting	129
17	Salghari	439	67	Chuba	200	117	Mangbrue	471
18	Dhargaon	209	68	Parbing	294	118	Tingmo	242
19	Dorop	277	69	Rameng	123	119	Sanghanath	126
20	Gom	329	70	Nijarmeng	460	120	Tinkitam	142
21	Sorok	357	71	Burul	110	121	Rayong	149
22	Shyampani	119	72	Bamyak	230	122	Sangmo	227
23	Sangbung	479	73	Thangsing	310	123	Ravong	629
24	Assangthang	344	74	Tokal	385	124	Sokpay	84
25	Kopchey	313	75	Tokdey	332	125	Lingi	322
26	Mikkhola	279	76	Gangchung	730	126	Lower Paiyong	319
27	Manpur	212	77	Aifaltar	241	127	Upper Paiyong	185
28	Kitam	490	78	Temi Tea Estate	1323.00	128	Kau	162
29	Kartickey	551	79	Temi	1004	129	Lingmo	85
30	Sumbuk	918	80	Tarku	493	130	Pepthang	275
31	Suntaley	187	81	Tanak	431	131	Kolthang	600
32	Rong	182	82	Pabong	330	132	Tokday	584
33	Palum	141	83	Doring	712	133	Mangzing	274
34	Singtam	208	84	Rashyap	1402	134	Neh-Brum	293
35	Bul	199	85	Namphing	1310	135	Sripatam	353
36	Bomtar	539	86	Tsalumthang	551	136	Namphok	389
37	Singhithang	125	87	Turung	222	137	Gagyong	692
38	Saleumbong	253	88	Kanamtek	314	138	Rangang	396
39	Phalidara	246	89	Pamphok	439	139	Yangyang	410
40	Maniram	392	90	Donok	430	140	Satam	280
41	Longchok	278	91	Mamring	2038	141	Namphrik	100
42	Kamarey	489	92	Temi Forest Block	-	142	Ben	263
43	Panchgharey	443	93	Namchi Forest Block	-	143	Deu	230
44	Turuk	254	94	Majhitar Forest Block	12	144	Lingmo Forest Block	-
45	Ramabong	287	95	Jorethang Forest Block		145	Yangyang Forest Block	-
46	Kerabari	448	96	Melli Forest Block	2	146	Ralang Forest Block	-

47	Melli	5734	97	Namthang Forest Block		147	Rabongla Forest Block	60
48	Mellidara	461	98	Mamring Forest Block	1	148	Kewzing Forest Block	-
49	Paiyong	370	99	Sada	64	149	Namchi (Town)	1705
50	Suntaley	309	100	Phamthang	123	150	Jorethang (Town)	20020

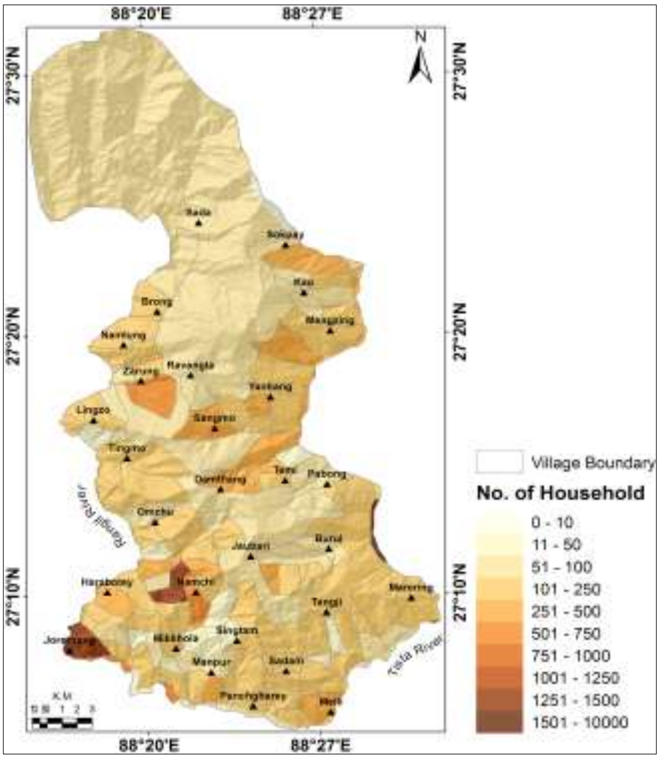

Fig. 6: Household distribution map of South Sikkim Himalaya (Indian census 2011)[46]

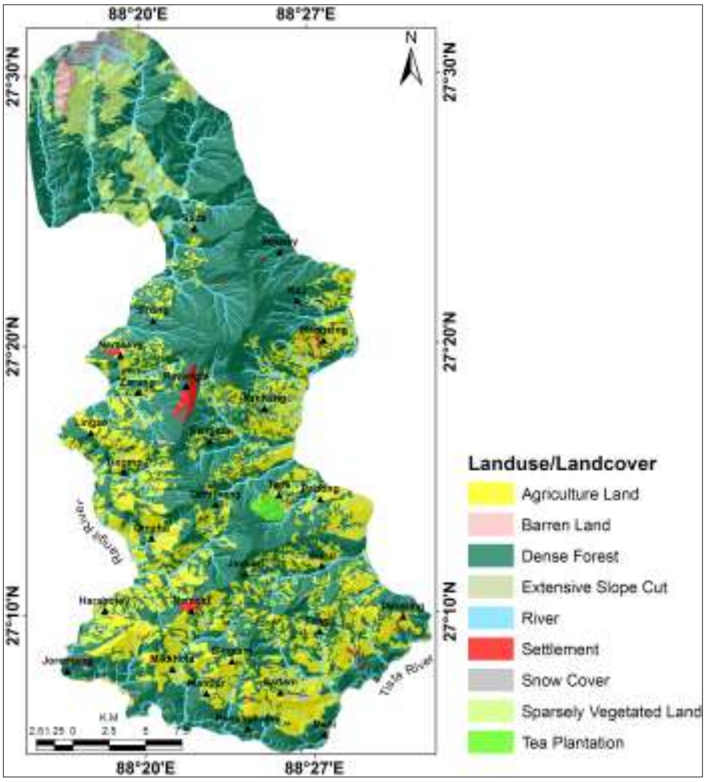

Fig. 7: Landuse/Landcover map of South Sikkim Himalaya

Table 3
Household distribution of South Sikkim Himalaya (Indian census 2011)[46]

S.N.	Name of Village	Number of Households	S.N.	Name of Village	Number of Households	S.N.	Name of Village	Number of Households
1	Omchu	96	50	Suntaley	239	99	Sada	27
2	Chumlok	154	51	Sukrabarey	262	100	Phamthang	126
3	Wak	154	52	Sadam	189	101	Brong	192
4	Chemchey	74	53	Rabitar	151	102	Poley	184
5	Damthang	126	54	Rabikhola	69	103	Namlung	192
6	Jaubari	124	55	Tangji	146	104	Lingdong	107
7	Tingrithang	112	56	Bikmat	131	105	Ralong	131
8	Mamley	206	57	Rateypani	252	106	Ralong Moastery	25
9	Pabong	127	58	Passi	96	107	Deythang	206
10	Pajer	39	59	Kateng-Bokrang	195	108	Zarung	177
11	Kamrang	311	60	Paleytam	47	109	Barfung	927
12	Tinzer	55	61	Nalam-Kolbong	221	110	Bakkhim	193
13	Denchung	212	62	Nagi	194	111	Kewzing	89
14	poklok	363	63	Maneydara	189	112	Dalep	153
15	Tinik	190	64	Kabrey	180	113	Lingzo	157
16	Chisopani	299	65	Karek	226	114	Likship	595
17	Salghari	184	66	Phong	129	115	Hingdam	69
18	Dhargaon	81	67	Chuba	153	116	Lamting	70
19	Dorop	156	68	Parbing	347	117	Mangbrue	47
20	Gom	234	69	Rameng	116	118	Tingmo	273
21	Sorok	103	70	Nijarmeng	102	119	Sanghanath	207
22	Shyampani	43	71	Burul	79	120	Tinkitam	148
23	Sangbung	186	72	Bamyak	121	121	Rayong	144
24	Assangthang	168	73	Thangsing	97	122	Sangmo	331
25	Kopchey	168	74	Tokal	182	123	Ravong	353
26	Mikkhola	147	75	Tokdey	99	124	Sokpay	89
27	Manpur	44	76	Gangchung	131	125	Lingi	343
28	Kitam	213	77	Aifaltar	57	126	Lower Paiyong	136
29	Kartickey	161	78	Temi Tea Estate	247	127	Upper Paiyong	98
30	Sumbuk	240	79	Temi	278	128	Kau	75
31	Suntaley	94	80	Tarku	371	129	Lingmo	59
32	Rong	139	81	Tanak	182	130	Pepthang	73
33	Palum	40	82	Pabong	101	131	Kolthang	241
34	Singtam	57	83	Doring	254	132	Tokday	265
35	Bul	55	84	Rashyap	241	133	Mangzing	216
36	Bomtar	201	85	Namphing	581	13	Neh-Brum	306
37	Singhithang	74	86	Tsalumthang	173	135	Sripatam	256
38	Saleumbong	122	87	Turung	225	136	Namphok	250
39	Phalidara	171	88	Kanamtek	110	137	Gagyong	378
40	Maniram	222	89	Pamphok	211	138	Rangang	292
41	Longchok	193	90	Donok	60	139	Yangyang	272
42	Kamarey	173	91	Mamring	327	140	Satam	242
43	Panchgharey	192	92	Temi Forest Block	-	141	Namphrik	123
44	Turuk	226	93	Namchi Forest Block	-	142	Ben	448
45	Ramabong	179	94	Majhitar Forest Block	49	143	Deu	238

46	Kerabari	145	95	Jorethang Forest Block	-	144	Lingmo Forest Block	-
47	Melli	615	96	Melli Forest Block	14	145	Yangyang Forest Block	-
48	Mellidara	338	97	Namthang Forest Block	-	146	Ralang Forest Block	-
49	Paiyong	220	98	Mamring Forest Block	07	147	Rabongla Forest Block	123
						148	Kewzing Forest Block	-
						149	Namchi Town	2733
						150	Jorethang Town	2107

Table 4
Error matrix derived for landuse/landcover mapping of South Sikkim Himalaya.

		GPS based ground truth										
		Agriculture Land	**Barren Land**	**Dense Forest**	**Extensive Slope Cut**	**River/ Water bodies**	**Settle ment**	**Snow Cover**	**Sparsely Vegetated Land**	**Tea Plantation**	**Total**	**User's accuracy**
Satellite image (SENTINEL-2A) Based LULC (classified data)	Agriculture Land	27	2	1	0	0	7	0	3	4	44	61.3
	Barren Land	1	7	0	0	0	0	0	0	0	8	87.5
	Dense Forest	2	0	29	0	0	0	0	5	3	39	74.3
	Extensive Slope Cut	0	2	0	11	0	0	0	0	0	13	84.6
	River/ Water bodies	0	0	0	0	7	0	1	0	0	8	87.5
	Settlement	3	0	0	0	0	17	0	0	0	20	85
	Snow Cover	0	0	0	0	2	0	9	0	0	11	81.8
	Sparsely Vegetated Land	1	0	3	0	0	0	0	19	3	26	73.1
	Tea Plantation	4	0	1	0	0	0	0	5	21	31	67.7
	TOTAL	38	11	34	11	9	24	10	32	31		
	Producer Accuracy	71.1	63.6	85.2	100	77.7	70.9	90	59.3	67.7		
	Overall Accuracy	73.5										
	Kappa statistics	0.6911062										

Building typology: Types of building construction materials are significant features in assessing vulnerability of landslide hazard. In this study, Google Earth Imagery has been used for creation of building footprint map, thereafter high resolution multispectral data like SENTINEL-2A data has been used for identification of different types of buildings materials. In the present study, 'PCA' (Principal Component Analysis),'Textural Analysis' and 'Normalized Differences Building Index' (NDBI) have been achieved for the detection of building materials. Zha et al have used similar technology to identify building materials. The building materials have been categorized into 3 classes i.e. (i) building by field stone, rural structures, unbrick houses; light weight, (ii) ordinary burnt brick building-building of the large block and pre-bricated type; heavy weight, (iii) reinforced building; flat roof (concrete)' are followed according to BMTPC.[47] The building in field stone, rural structures, unbrick houses are dominated in South Sikkim Himalaya as depicted in fig. 8.

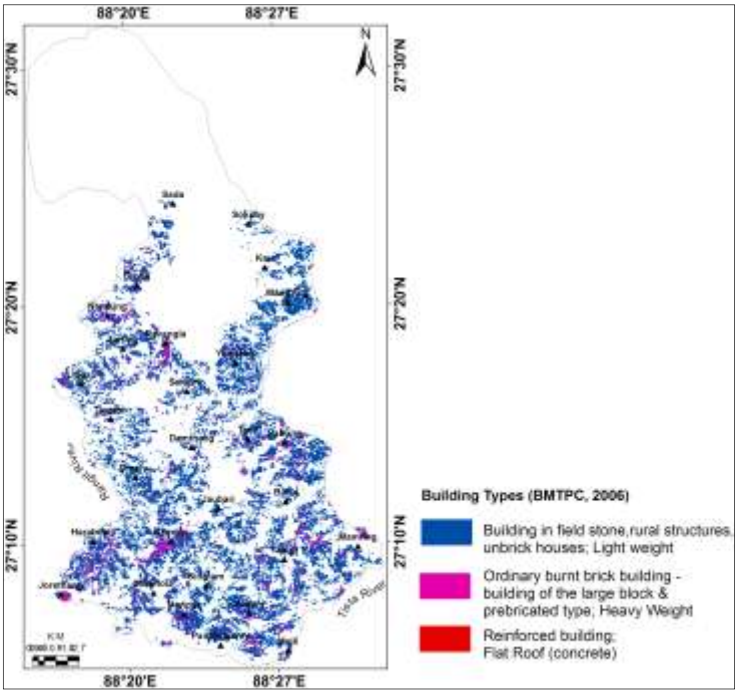

Fig. 8: Building typology distribution map of South Sikkim Himalaya derived using SENTINEL- 2A data

Table 5
Error matrix derived for building typology in South Sikkim Himalaya.

	Rapid Visual Screening based building height (reference data)					**User's accuracy**
		Building in field stone, rural structures	**Ordinary burnt brick building - building of the large block & prebricated type; Heavy Weight**	**Reinforced building; Flat Roof (concrete)**	**Total**	
Google Earth 3D aspect based building height (classified data)	Building in field stone, rural structures	71	17	9	97	73.19587629
	Ordinary burnt brick building - building of the large block & prebricated type; Heavy Weight	11	55	2	68	80.88235294
	Reinforced building; Flat Roof (concrete)	3	5	27	35	77.14285714
		85	77	76		
	Producer's accuracy	83.5294	71.42857143	35.5263157		
	Overall Accuracy	76%				
	Kappa Statistics	0.626821231				

In the table 5, the accuracy assessment between the 'reference' (RVS derived) and 'classified' (SENTINEL-2A derived) maps has been discussed.

Building Height: In the current investigation, Google Earth and 200 ground truth GCP have been utilized for visual detection of building height utilizing 3D feature and its validation. Building height map of the South Sikkim Himalaya is introduced in fig. 9. The overall accuracy statistics of the RVS derived reference and the Google Earth derived classified maps have been presented in table 6. The building heights have been categorized into four classes i.e. 1 floor houses, 2 to 4 floors buildings, 5 to 7 floors tall buildings, above 7 floors multi-storeyed buildings.

Building Density: Building density is one of the most important attributes in evaluating vulnerability to landslide hazard. In the present study, SENTINEL-2A data has been used to make building density map. The building density is categorized into 10 classes i.e. no data, 1 to 10 buildings per sq. km., 11 to 25 buildings per sq. km., 26 to 50 buildings per sq. km., 51 to 75 buildings per sq. km., 76 to 100 buildings per sq. km., 101 to 200 buildings per sq. km., 201 to 300 buildings per sq. km., 301 to 400 buildings per sq. km. and 401 to 784 buildings per sq. km. High altitude areas are located in the northern part of the South Sikkim Himalaya. This area is also covered with dense forest.

Apart from this, throughout the year some part of this area is covered with snow due to which no settlement has been found in the northern part of this study area. Therefore, no data is available in regard to building density. The building density is high in Namchi, Jorethang, Melli and Ravangla area (Fig. 10).

Table 6
Error matrix derived for building height in South Sikkim Himalaya

	Rapid Visual Screening based building height (reference data)						User's accuracy
		1 floor	2-4 floor	5-7 floor	>7 floor	Total	
Google Earth 3D aspect based building height (classified data)	1 floor	67	7	3	0	77	87.01299
	2-4 floor	7	45	5	1	58	77.58621
	5-7 floor	2	3	32	4	41	78.04878
	>7 floor	0	2	5	17	24	70.83333
	Total	76	57	45	22		
	Producer's accuracy	88.1578947	78.947	71.1111	77.2727		
	Overall Accuracy	80.5 %					
	Kappa Statistics	0.72602					

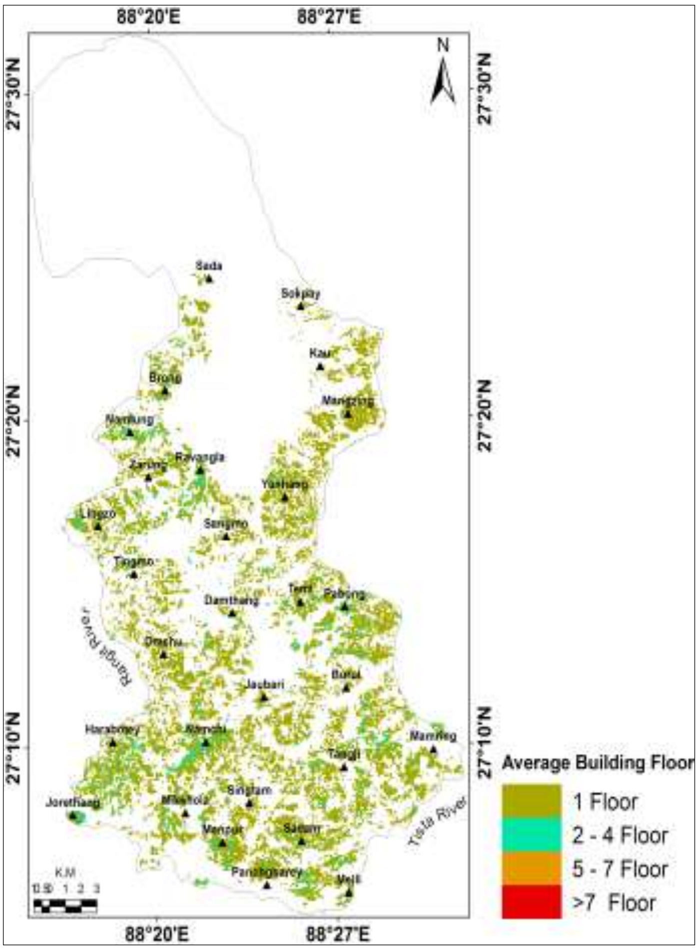

Fig. 9: Building height map of South Sikkim Himalaya

Analytical Hierarch Process (AHP) and landslide risk: Analytical Hierarchy Process (AHP) method is a multi criteria decision- making (MCDM) model used to determine the judgment on the instability rank of the factors by assessing weights/ eigenvector. AHP method proposed by Saaty[25] is very popular for decision making. In AHP method a pair wise comparison matrix is formed to explain hierarchical structure of multiple criteria in decision making. With the help of AHP method, quantitative and qualitative information regarding decision making study can be prepared. An equal number of rows and columns are comprised in pair wise comparison matrix, where values are placed on one side of the diagonal, whereas values of 1 are recorded in the diagonal of the matrix[48].

To make a pair-wise comparison matrix, each factor/themes is rated against each other factor by designating a relative dominant scale between 1 and 9 (Table 7) and such scale is known as a preference scale, where value 1 indicates ‘‘ equal importance ’’ between two factors and the value 9 indicates the ‘‘extreme importance ’’ of one factor compared to other[49].

The value also extends among the reciprocals 1/2 and 1/9 for opposite comparison. After creating a pair-wise comparison matrix in the AHP model, it is normalized and then the weighted value of each factor is determined. Whether the pair-wise comparison matrix in AHP model is consistent or not, is judged by Consistency Ratio (CR).

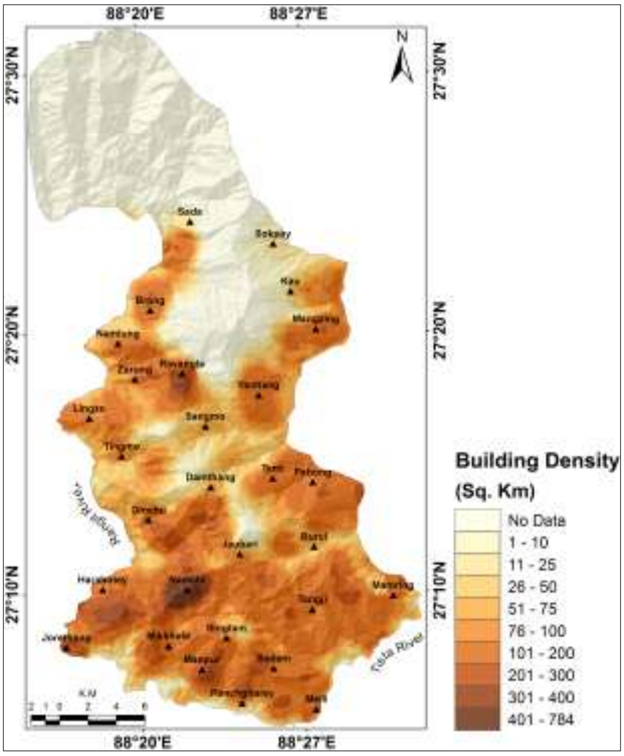

Fig. 10: Building density map of South Sikkim Himalaya using Google Earth

Table 7
Scale of preference between two parameters[49]

Scale	Degree of preference	Explanation
1	Equally	Two activities contribute equally to the objective.
3	Moderately	Experience and judgment slightly to moderately favors one activity over another.
5	Strongly	Experience and judgment strongly or essentially favour one activity over another.
7	Very Strongly	An activity is strongly favored over another and its dominance is showed in practice.
9	Extremely	The evidence of favoring one activity over another is of the highest degree possible of an affirmation.
2, 4, 6 and 8	Intermediate values	Used to represent compromises between the references in weight 1, 3, 5, 7 and 9.
Reciprocals	Opposites	Used for inverse comparison.

In this study selected spatial vulnerability exposures (building height, building typology and building density) and non spatial vulnerability exposures (population density, landuse/ landcover, household distribution) have been taken to calculate landslide induced socio-economic and structural risk. Two separate pair-wise comparison matrix have been developed with the help of AHP model to determine socio-economic and structural risk and using the following steps they have been normalized and the weighed value of each factor has been determined[50].

(i) Using this formula, the value of each column of the pair-wise comparison matrix is added (Table 8 and 9)

$$L_j = \sum C_{ij} \quad (5)$$

where L_j denotes the sum of each column of the pair- wise comparison matrix and C_{ij} denotes the value assigned to each factor at ith row and jth column.

(ii) Divide every value of the factor in the matrix by its column total to make a normalized pair-wise comparison matrix (Table 10 and 11).

$$X_{ij} = \frac{C_{ij}}{L_j} \quad (6)$$

where X_{ij} denotes the value at ith row and jth column in the pair-wise comparison matrix.

Table 8
Pair-wise comparison matrix of the data layers used for calculate socio-economic risk

	LHI	**LULC**	**No. Of Household**	**Population Density**
LHI	1	2	3	4
LULC	0.5	1	2	3
No. Of Household	0.33	0.5	1	2
Population Density	0.25	0.33	0.5	1
Total	2.08	3.83	6.5	10

Table 9
Pair-wise comparison matrix of the data layers used for calculate structural risk

	LHI	**Building Type**	**Building Height**	**Building Density**
LHI	1	2	3	4
Building Type	0.5	1	2	3
Building Height	0.33	0.5	1	2
Building Density	0.25	0.33	0.5	1
Total	2.08	3.83	6.5	10

Table 10
Normalized Pair-wise comparison matrix and weights of the data layers used for calculate socio-economic risk

	LHI	**LULC**	**No. Of Household**	**Population Density**	**Normalized Weight**
LHI	0.48	0.52	0.46	0.4	0.46
LULC	0.24	0.26	0.30	0.3	0.26
No. Of Household	0.16	0.13	0.15	0.2	0.14
Population Density	0.12	0.86	0.08	0.1	0.14

Table 11
Normalized Pair-wise comparison matrix and weights of the data layers used for calculate socio-economic risk

	LHI	**Building Type**	**Building Height**	**Building Density**	**Normalized Weight**
LHI	0.48	0.52	0.46	0.4	0.46
Building Type	0.24	0.26	0.31	0.3	0.26
Building Height	0.16	0.13	0.15	0.2	0.14
Building Density	0.12	0.86	0.08	0.1	0.14

(iii) Using this formula, divide the total value of the normalized row of the matrix by the number of factors used (N) to produce standard weights.

$$W_i = \frac{\sum X_{ij}}{N} \tag{7}$$

where W_i denotes standard weight.

Using matrix multiplication, consistency vector (λ) has been calculated by multiply the pair-wise comparison matrix values and normalized pair-wise matrix[50].

(iv) Following formula has been used to calculate consistency vector (λ)

$$\lambda = \sum (C_{ij} X_{ij}) \tag{8}$$

where λ denotes consistency vector.

(v) Consistency Index (CI) has been calculated by using the following formula.

$$CI = \frac{\lambda - n}{n - 1} \tag{9}$$

where CI denotes Consistency Index, n denotes Number of factors used.

(vi) Following formula has been used to calculate Consistency Ratio (CR):

$$CR = \frac{CI}{RI} \tag{10}$$

where RI denotes Random Inconsistency.[25]

If the value of Consistency Ratio (CR) is less than or equal to 0.1, the inconsistency is satisfactory, but if the Consistency Ratio is greater than 0.1, then there is need to revise subjective judgement[49].

The related attributes have been ranked within the factors (spatial and non spatial exposures) and the ranks have also been normalized using the following formula[51]:

$$X_j = \frac{R_j - R_{\min}}{R_{\max} - R_{\min}} \tag{11}$$

where R_j denotes row score, $R_{\max}$ and $R_{\min}$ represent the maximum and minimum scores of a particular factors.

Socio-economic risk Assessment: The socio-economic risk elements i.e. population density, household distribution and land use/land cover have been integrated over the Landslide Susceptibility Index (LSI) to delineate the most vulnerable zones in terms of socio-economic activities of the study area. The socio-economic risk index (SERI) has been calculated using the following equation.

$$\text{SERI} = (\text{LSI}_w \text{LSI}_r + \text{PD}_w \text{PD}_r + \text{HH}_w \text{HH}_r + \text{LULC}_w \text{LULC}_r) / \sum W \tag{12}$$

where LSI denotes Landslide Index, PD is Population Density, HH is Household distribution and LULC is landuse and landcover and W are Weights.

The ranks and weights for socio- economic vulnerability exposures over landslide hazard zonation have been explained in table 12. The perception of social vulnerability helps to recognize those characteristics and experiences of individuals and communities that facilitate them to react and recover from landslide hazards.

Structural risk Assessment: The structural risk elements i.e. building typology, building height and building density have been incorporated over the Landslide Susceptibility Index (LSI) to prepare Structural Risk Index(SRI) .The Structural Risk Index (SRI) has been calculated using the following equation.

$$\text{SRI} = (\text{LSI}_w \text{LSI}_r + \text{BT}_w \text{BT}_r + \text{BH}_w \text{BH}_r + \text{BD}_w \text{BD}_r) / \sum W \tag{13}$$

where LSI denotes Landslide Index, BT is Building Typology, BH is Building Height and BD is Building Density, W are Weights.

The ranks and weights for structural vulnerability exposures over Landslide Susceptibility Index are explained in table 13.

Results and Discussion

Analysis of Landslide Susceptibility: Independent variables associated with causative factors and the position of the dependent variable (i.e. landslide present or absent) have been taken into account for measuring BLR coefficients (Eq.2) for each pixel. In the regression analysis, an equal number of samples for the presence and absence of landslide has been considered. In the South Sikkim Himalaya, 346 pixels (12.5m×12.5m) have been identified as landslide affected. Therefore, 70% of landslide pixels (i.e. 242 pixels) have been arbitrarily selected and rest is kept for accuracy estimation. Besides, another set of 346 random pixels have been selected from landslide free areas.

Similarly, 70% of these have been applied for modelling and rest is used for accuracy evaluation. In the regression analysis, an equal number of samples for the presence and absence of landslide has been considered. A tabular database has been organized for model development which it contains values of 14 independent variables along with a binary data regarding landslide presence or absence having 484 pixels.

On the basis of landslide histogram analysis, the categorical variables are also measured as a continuous variable. The forward stepwise method of variable selection was ended at iteration number 5 because parameter assessment changed by less than .001 (Table 14).

All the reserved independent variables have the estimated coefficients (β_i) statistically different from 0. The null hypothesis used to test is that the coefficients of the independent variable (β_i) is 0. The Wald chi-square (χ^2) value (Eq.3) at 5 % significance level for the corresponding degree of freedom (df) has been used to test the hypothesis[52]:

$$\chi^2 = \left(\frac{\beta_1}{SE}\right)^2 \quad (7)$$

where S.E. is the standard error and is given as SE=(s/$\sqrt{n}$), s is the standard deviation of the input data.

In this study, a logistic regression equation has been achieved as shown in eq. 8:

Table 12
Normalized weights and ranks assigned to respective themes and the attributes of socio-economic risk attributes for thematic integration on GIS

Themes	Attributes	Rank	Normalized Rank	Weight
Landslide Hazard Index and socio- economic landslide vulnerability exposures				
Landslide Hazard Index (LHI)	Low	1	0	0.46
	Medium	2	0.3333	
	High	3	0.6666	
	Severe	4	1	
LULC	Barren Land	1	0	0.26
	River/Water bodies	2	0.125	
	Dense Forest	3	0.25	
	Extensive Slope Cut	4	0.375	
	Sparsely Vegetated Land	5	0.5	
	Tea Plantation	6	0.625	
	Snow Cover	7	0.75	
	Agriculture Land	8	0.875	
	Settlement	9	1	
No. Of Household	0-10	1	0	0.14
	11-50	2	0.111111111	
	51-100	3	0.222222222	
	101-250	4	0.333333333	
	251-500	5	0.444444444	
	501-750	6	0.555555556	
	751-1000	7	0.666666667	
	1001-1250	8	0.777777778	
	1251-1500	9	0.888888889	
	1501-10000	10	1	
Population Density	0-25	1	0	0.14
	26-50	2	0.111111111	
	51-100	3	0.222222222	
	101-200	4	0.333333333	
	201-300	5	0.444444444	
	301-400	6	0.555555556	
	401-500	7	0.666666667	
	501-1000	8	0.777777778	
	1001-1500	9	0.888888889	
	1501-2134	10	1	

Table 13
Normalized weights and ranks assigned to respective themes and the attributes of structural risk for thematic integration on GIS

Themes	Attributes	Rank	Normalized Rank	Weight
Landslide Hazard Index and structural landslide vulnerability exposures				
Landslide Hazard Index (LHI)	Low	1	0	0.46
	Medium	2	0.3333	
	High	3	0.6666	
	Severe	4	1	
Building Type	Reinforced building;Flat Roof (concrete)	1	0.000000	0.26
	Ordinary burnt brick building -building of the large block & prebricated type; Heavy Weight	2	0.500000	
	Building in field stone,rural structures, unbrick houses:light weight	3	1.000000	
Building Height	1 floor	1	0.000000	0.14
	2-4 floor	2	0.333333	
	5-7 floor	3	0.666667	
	>7 floor	4	1.000000	
Building Density	1-10	1	0.000000	0.14
	11-25	2	0.125000	
	26-50	3	0.250000	
	51-75	4	0.375000	
	76-100	5	0.500000	
	101-200	6	0.625000	
	201-300	7	0.750000	
	301-400	8	0.875000	
	401-784	9	1.000000	

Table 14
Estimation of co-efficient through BLR model

Parameters	B	S.E.	Wald	df	Sig.	Exp(B)
Aspect	1.529	.374	16.704	1	.000	4.615
Elevation	.743	.518	2.059	1	.151	2.102
Earthquake proximity	-1.493	2.070	.520	1	.471	.225
Geology	-.275	1.003	.075	1	.784	.759
Geomorphology	1.783	.827	4.646	1	.031	5.948
Lineament density	.837	.677	1.526	1	.217	2.309
Lineament distance	.253	.716	.125	1	.724	1.288
Landuse/ landcover	-.111	1.109	.010	1	.920	.895
Rainfall	4.152	1.238	11.244	1	.001	63.580
River density	.420	.658	.407	1	.523	1.522
River distance	.809	.623	1.688	1	.194	2.246
Road density	1.329	.856	2.412	1	.120	3.778
Road distance	1.287	.712	3.268	1	.071	3.624
Slope	2.019	.479	17.761	1	.000	7.534
Constant	-5.780	2.188	6.980	1	.008	.003

$$Z = -5.780 + (1.529 * [\text{aspect}]) + (.743 * [\text{elevation}]) + (-1.493 * [\text{earthquake proximity}]) + (-.275 * [\text{geology}]) + (1.783 * [\text{geomorphology}]) + (.837 * [\text{lineament density}]) + (.253 * [\text{lineament distance}]) + (-.111 * [\text{lulc}]) + (4.152 * [\text{rainfall}]) + (.420 * [\text{river density}]) + (.809 * [\text{river distance}]) + (1.329 * [\text{road density}]) + (1.287 * [\text{road distance}]) + (2.019 * [\text{slope}]) \quad (8)$$

Nagelkerke R square value for 5^{th} iteration is found to be 0.276, confirming that the statistical model supports the validity of the system with these variables. The overall system has a success of classifying 69% of the pixel correctly (Table 15).

BLR analysis developed the estimates of constant and the coefficients of independent variables. Positive logistic coefficient gives a signal that the independent variable raises the probability of a landslide and the negative values decrease the probability of landslide occurrence[53]. The predicted probability of landslide for the whole study area has been calculated using eq. 1.

The corresponding predicted probability map is depicted by numbers existing between 0 and 1. In this map, the pixel value close to 1 suggests higher probability of landslide whereas the value close to 0 indicates low probability. After reclassification, the landslide susceptibility map has been comprised with four equal susceptibility zones viz. severe, high, moderate and low landslide susceptibility (Fig.11).

Geospatial technology has acted a significant role to develop all data layers in the present work. A comprehensive study of 14 independent variables through the binary logistic regression model noticeably explains that due to highest exponential value (β_i), the rainfall acts a very significant function in determining the stability of slopes in South Sikkim Himalaya.

In South Sikkim Himalaya, slope was regarded as the 2^{nd} highest positive effects of slope instability assigned by the coefficient and its exponential value. Geomorphology has positive coefficient and 3^{rd} highest exponential value acts a very vital role in deciding the stability of the slope in the study area. The approximate coefficient of lineament density reveals positive value which indicates where lineament density is higher, the probability of landslide is also higher. The distance to deduce lineaments and the distance to drainage show an inverse relationship with slope failure. Hence with the increase of distance, their impact towards slope instability decreases[54].

Table 15
Classification summary of the logistic regression model

Observe		Predicted		
		Landslide		
		0	1	Percentage Correct
Landslide	0	168	76	68.9
	1	76	163	68.2
	Overall Percentage			68.5

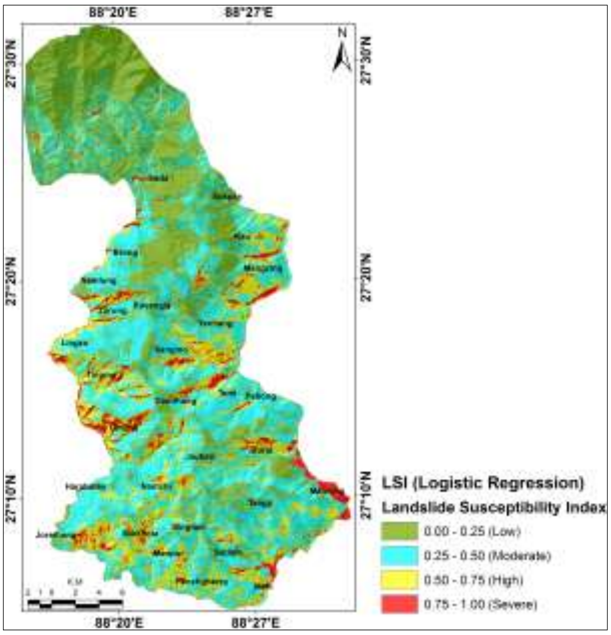

Fig. 11: Landslide susceptibility zonation map of South Sikkim Himalaya

Road density, road distance, slope aspect and elevation show relatively high exponential value (β_i), indicating its ability to slope failure, which can promote landslides occurrences. Through BLR method landslide susceptibility zone map has been produced and correlated with the prevailing landslide distribution layer. On the basis of BLR method, landslide density of predicted susceptibility zonation map has been made (Table 16).

It can be said that 23.77% of the observed landslides fall in 4.5% of the predicted severe susceptibility zone and this situation is found in the study area. 26.85% is classified into low susceptible zone having low landslide density of 5.81.

According to BLR model, landslide susceptibility zonation map has been prepared and classified into four susceptibility groups such as severe, high, moderate andlow. Melli, Mamring, Mikkhola, Jorethang, Namchi, Jaubari, Damthang, Mangzing, Omchu, Tingmo, Sada and Ravangla areas of South Sikkim Himalaya fall in severe landslide susceptibility zone. High landslide susceptibility is observed in southern, eastern and south-western part of this study area. Moderate landslide susceptibility has been registered throughout the study area except extreme northern part of the study area. Low landslide susceptibility is observed in the northernmost part of the study area and in some parts of the central part.

Integration of landslide susceptibility map and landslide vulnerability exposures through Analytical Hierarchy process: Analytical Hierarchy Process (AHP) is generally used to assigned suitable weights on landslide causative factors according to their relative importance. To assess socio-economic and structural risk, five landslide vulnerability exposures have been taken and using Analytical Hierarchy Process landslide susceptibility map has been integrated with vulnerability exposures maps. In this study AHP method has been used to assign the weights of different vulnerability exposures and landslide hazard zonation for calculate socio- economic and structural risk.

For calculation of socio- economic and structural risk, two different pair wise comparison matrix have been determined and normalized. A consistency ratio has also been calculated to decide that two different AHP matrix is consistent or not (Table 17).

The consistency ratio of socio-economic risk has been calculated by dividing consistency index (CI) by random inconsistency value (RI). Random inconsistency values (RI) are shown in table 18. In this study the consistency ratio of socio-economic risk is 0.09 which is less than 0.1, hence the inconsistency of pair-wise comparison matrix of socio-economic risk is acceptable.

The numbers of themes are four in both pair-wise comparison matrix of socio-economic and structural risk, therefore consistency ratio of structural risk will be equal to the consistency ratio of socio-economic risk.

Table 16
Landslide density in predicted susceptibility zone based on BLR method.

Landslide susceptibility zones	Percentage area of predicted zones	Percentage area of observed landslide in each zones (b)	Landslide density (b/a)
Low	26.81	5.81	0.22
Moderate	48.56	27.03	0.56
High	20.08	39.83	1.98
Severe	4.55	27.33	6.01

Table 17
Consistency ratio of socio-economic risk

	LHI	LULC	No. of Household	Population Density	Weighted Sum (WS)	Normalized Weight (NW)	WS/NW	Consistency vector (λ)	$CI = \frac{\lambda - n}{n-1}$	$CR = \frac{CI}{RI}$
LHI	0.46	0.52	0.42	0.56	1.96	0.46	4.26	4.245	0.0812	0.09
LULC	0.23	0.26	0.28	0.42	1.19	0.26	4.58			
No. of Household	0.15	0.13	0.14	0.28	0.7	0.14	5			
Population Density	0.12	0.09	0.07	0.16	0.44	0.14	3.14			

Table 18
Random index value[49]

n	1	2	3	4	5	6	7	8	9	10
RI	0.0	0.0	0.58	0.90	1.12	1.24	1.32	1.41	1.45	1.49

Landslide Risk Analysis of South Sikkim Himalaya: Socio-economic risk map of South Sikkim Himalaya has been depicted in fig. 12. The socio-economic risk index (SERI) map has been classified into four such as severe, high, medium and low. Severe risk landslide dominated areas are Jorethang, Melli and part of Namchi, Mikkhola, Yangyang and Temi. South, South-West and Eastern part of the study area are experienced with High risk landslide condition. Middle part and some small patches throughout the study area are registered with medium risk landslide condition. Northern part and also some small patches all over of South Sikkim Himalaya are characterised by low landslide risk condition.

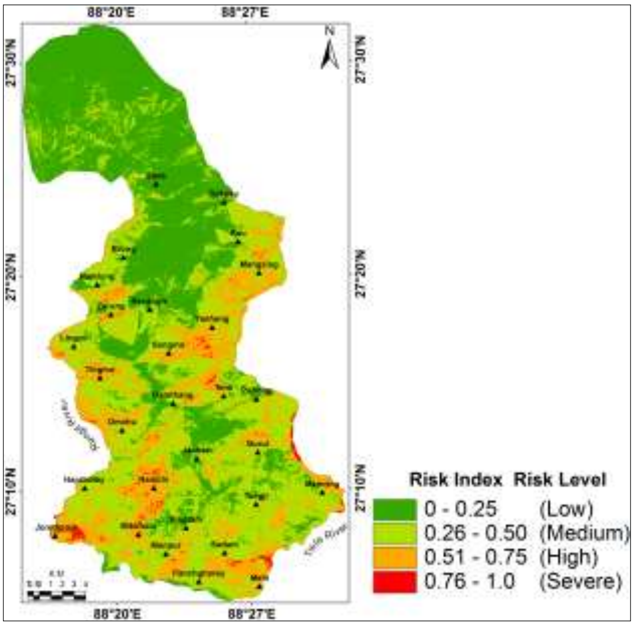

Fig. 12: Landslide socio-economic risk map of South Sikkim Himalaya

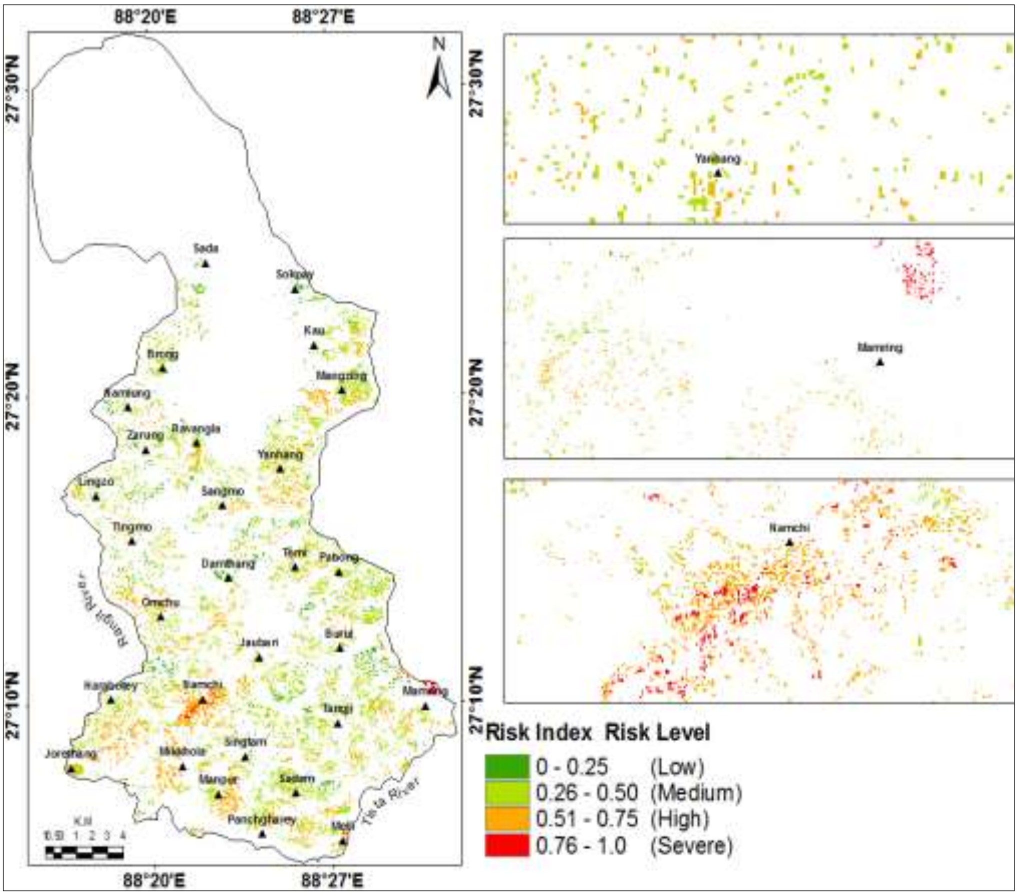

Fig. 13: Landslide structural risk map of South Sikkim Himalaya

The most and least structural vulnerable areas have been identified on the basis of SRI scores. The range of SRI scores varies from <0.25 (low vulnerability) to 1 (high vulnerability) (Fig.13). Structural Risk Index (SRI) has been divided into four and identified as severe, high, medium and low risk. Severe structural risk dominated areas are Namchi, Mamring, Melli, Jorethang and Manpur. Namchi is the district head quarter of South district of Sikkim. Jorethang and Melli are the growing town of South Sikkim Himalaya and although Manpur and Mamring are two villages but they are located near the towns of Namchi and Rangpo. South,

South-West and Eastern part of the study area are dominated by high structural risk condition. The entire study area apart from Northern part is dominated by medium structural risk condition while SRI <0.25 (low vulnerability) presents a completely risk free regime. It is easier to identify from the landslide structural risk map, the most vulnerable buildings and therefore it will be feasible to take proper preventive measures.

Conclusion

Landslide vulnerability and risk have appeared as significant subject in densely populated mountainous area. The landslide risk framework is a multifaceted concept based on landslide hazard. Physiographic and anthropogenic database and the vulnerability exposures viz. population density, house hold distribution, land use/land cover, building typology, building height and building density have been carefully incorporated on GIS to recognize landslide related socio-economic and structural risk conditions of South Sikkim Himalaya.

It has been identified from population density, house hold distribution and building density vulnerability exposures map and two landslide risk map viz. socio-economic risk map and structural risk map that with the increase of population density, house hold distribution and building density, the landslide risk has been increased. Hence there is a direct relationship between above mentioned vulnerability exposures and landslide risk.

Simultaneously it has been identified that the landslide risk has increased with the increase of building's height. Building typology exposures map shows that building material also determined the magnitude of landslide risk. Ordinary burnt brick building- building of the large block and prebricated type and heavy weight are more vulnerable to landslide. In South Sikkim Himalaya about 40% area falls under the high risk zone. Namchi, Mamring, Melli, Jorethang, Manpur and Yangyang are in severe risk zone. Both the socio-economic and structural risk maps are expected to play important roles in landslide impose disaster mitigation and management of the South Sikkim Himalaya.

References

1. Anabalagan R., Landslide hazard evaluation and zonation mapping in mountainous terrain, *Eng Geol*, **2**, 269–277 **(1992)**

2. Anbalagan R., Kumar R., Lakshmanan K., Parida S. and Neethu S., Landslide hazard zonation mapping using frequency ratio and fuzzy logic approach, a case study of Lachung Valley, Sikkim, *Geoenviron Disasters*, **2(1)**, 6 **(2015)**

3. Rowbotham D. and Dudycha D.N., GIS modelling of slope stability in Phewa Tal watershed, *Nepal Geomorphology*, **26**, 151–170 **(1998)**

4. Lei Z. and Jing-feng H., GIS-based logistic regression method for landslide susceptibility mapping in regional scale, *Journal of Zhejiang University Science*, **7**, 2007–2017 **(2006)**

5. Lee S. and Pradhan B., Landslide hazard mapping at Selangor, Malaysia using frequency ratio and logistic regression models, *Landslides*, **4(1)**, 33–41 **(2007)**

6. Lee S., Ryu J.H., Won J.S. and Park H.J., Determination and publication of the weights for landslide susceptibility mapping using an artificial neural network, *Eng Geol.*, **71**, 289–302 **(2004a)**

7. Sarkar S. and Kanungo D.P., An integrated approach for landslide susceptibility mapping using remote sensing and GIS, photogram, *Engineering & Remote Sensing*, **70(5)**, 617–625 **(2004)**

8. Donati L. and Turrini M.C., An objective and method to rank the importance of the factors predisposing to landslides with the GIS methodology, application to an area of the Apennines (Valnerina; Perugia, Italy), *Engineering Geology*, **63**, 277–289 **(2002)**

9. Pandey A., Dabral P.P., Chowdhary V.M. and Yadav N.K., Landslide hazard zonation using remote sensing and GIS: a case study of Dikrong river basin, Arunachal Pradesh, India, *Environmental Geology*, **54**, 1517–1529 **(2008)**

10. Nithya E.S. and Prasanna R.P., An integrated approach with GIS and remote sensing technique for landslide zonation, *International Journal of Geomatics Geosciences*, **1(1)**, 66–75 **(2010)**

11. Pradhan B. and Lee S., Delineation of landslide hazard areas on Penang Island, Malaysia, by using frequency ratio, logistic regression and artificial neural network models, *Environmental Earth Sciences*, **60(5)**, 1037–1054 **(2010a)**

12. Pradhan B. and Lee S., Landslide susceptibility assessment and factor effect analysis: backpropagation artificial neural networks and their comparison with frequency ratio and bivariate logistic regression modelling, *Environmental Modelling & Software*, **25(6)**, 747–759 **(2010b)**

13. Guzzetti F., Carrara A., Cardinali M. and Reichenbach P., Landslide hazard evaluation: a review of current techniques and their application in a multi-scale study, Central Italy, *Geomorphology*, **31**, 181–216 **(1999a)**

14. Guzzetti F., Cardinali M., Reichenbach P. and Carrara A., Comparing landslide maps: a case study in the upper Tiber River basin, Central Italy, *Environmental Management*, **25(3)**, 247-363 **(1999b)**

15. Guzzetti F., Cardinali M., Reichenbach P. and Carrara A., Landslide hazard evaluation: an aid to a sustainable development, *Geomorphology*, **31**, 181–216 **(1999c)**

16. Jibson W.R., Edwin L.H. and John A.M., A method for producing digital probabilistic seismic landslide hazard maps, *Engineering Geology*, **58**, 271–289 **(2000)**

17. Ghosh S., Van Westen C.J., Carranza E. and Jetten V., Generation of event- based landslide inventory maps in a data-scarce environment; case study around Kurseong, Darjiling district, West Bengal, India, In Malet J.P., Remaitre A. and Bogaard T., eds., Landslide processes: from geomorphologic mapping to dynamic modelling: proceedings of the landslide processes, European Centre on geomorphological hazards (CERG), 37–44 **(2009)**

18. Atkinson P.M. and Massari R., Generalized linear modelling of susceptibility to landsliding in the central Apennines, Italy, *Computers & Geosciences*, **24**, 373–385 **(1998)**

19. Gokceoglu C., Sonmez H. and Ercanoglu M., Discontinuity controlled probabilistic slope failure risk map of the Altindag (settlement) region in Turkey, *Engineering Geology*, **55**, 277–296 **(2000)**

20. Dai F.C. and Lee C.F., Landslide characteristics and slope instability modelling using GIS; Lantau Island, Hong Kong, *Geomorphology*, **42**, 213–228 **(2002)**

21. Ohlmacher C.G. and Davis J.C., Using multiple logistic regression and GIS technology to predict landslide hazard in northeast Kansas, USA, *Engineering Geology*, **69**, 331-343 **(2003)**

22. Tasser E., Mader M. and Tappeiner U., Effects of land use in alpine grasslands on the probability of landslides, *Basic & Applied Ecology*, **4(3)**, 271-280, doi:10.1078/1439-1791- 00153 **(2003)**

23. Van Den Eeckhaut M., Vanwalleghem T., Poesen J., Govers G., Verstraeten G. and Vandekerckhove L., Prediction of landslide susceptibility using rare events logistic regression: A case-study in the Flemish Ardennes (Belgium), *Geomorphology*, **76**, 392–410 **(2006)**

24. Yesilnacar E. and Topal T., Landslide susceptibility mapping: A comparison of logistic regression and neural networks methods in a medium scale study, Hendek region, Turkey, *Engineering Geology*, **79(3-4)**, 251-266, doi:10.1016/j.enggeo.2005.02.002 **(2005)**

25. Saaty T.L., The analytical hierarchy process, McGraw Hill, New York, 350 **(1980)**

26. Yagi H., Development of assessment method for landslide hazardness by analytical hierarchy process (AHP), Abstract volume of the 42nd annual meeting of the Japan Landslide Society, 209–212 **(2003)**

27. Komac M., A landslide susceptibility model using the analytical hierarchy process method and multivariate statistics in perialpine Slovenia, *Geomorphology*, **74**, 17–28 **(2006)**

28. Kamp U., Growley B.J., Khattak G.A. and Owen L.A., GIS based landslide susceptibility mapping for the 2005 Kashmir earthquake region, *Geomorphology*, **101**, 631–642 **(2008)**

29. Yalcin A. and Bulut F., Landslide susceptibility mapping using GIS and digital photogrammetric techniques: a case study from Ardesen (NE Turkey), *Natural Hazard*, **41(1)**, 201–226 **(2007)**

30. Murmu P., Kumar M., Lal D., Sonkar I. and Singh S.K., Delineation of groundwater potential zones using geospatial techniques and analytical hierarchy process in Dumka district, Jharkhand, India, *Groundwater for Sustainable Development*, https://doi.org/10.1016/j.gsd.2019.100239 **(2019)**

31. Kanungo D.P., Arora M.K., Sarkar S. and Gupta R.P., A comparative study of conventional, ANN black box, fuzzy and combined neural and fuzzy weighting procedures for landslide susceptibility zonation in Darjeeling Himalayas, *Engineering Geology*, **85**, 347–366 **(2006)**

32. Bhandari R.K., The Indian landslide scenario: strategic issues and action points, *Disaster & Development*, **1(2) (2007)**

33. Mandal S. and Maiti R., Role of lithological composition and lineaments in land sliding: A case study of Shivkhola Watershed, Darjeeling Himalaya, *International Journal of Geology, Earth and Environmental Sciences*, **4(1)**, 126–132 **(2014)**

34. Bhattacharya S.K., The Study of Paglajhora Landslide in the Darjeeling Hills, West Bengal, India, *Indian Journal of Spatial Science*, **4(1)**, 21-27 **(2013)**

35. Mandal S.P., Chakrabarty A. and Maity P., Comparative evaluation of information value and frequency ratio in landslide susceptibility analysis along national highways of Sikkim Himalaya, *Spatial Information Research*, **26(2)**, 127–141 **(2018)**

36. Bera A., Mukhopadhyay B.P. and Das D., Landslide hazard zonation mapping using multi‑criteria analysis with the help of GIS techniques: a case study from Eastern Himalayas, Namchi, South Sikkim, *Natural Hazards*, **96(2)**, 935-959 **(2019)**

37. Basu T. and Pal S., A GIS‑based factor clustering and landslide susceptibility analysis using AHP for Gish River Basin, India, *Environment, Development and Sustainability*, **22**, 4787-4819 **(2019)**

38. Sarkar S., Kanungo D.P., Patra A.K. and Kumar P., GIS based spatial data analysis for landslide susceptibility mapping, *Journal of Mountain Science*, **5(1)**, 52-62 **(2008)**

39. Dasgupta S., Pande P., Ganguly D., Iqbal Z., Sanyal K., Venkatraman N.V., Dasgupta S., Sural B., Harendranath L., Mazumdar K., Sanyal S., Roy A., Das L.K., Misra P.S. and Gupta H., Seismotectonic atlas of India and its environs, Narula P.L., Acharyya S.K. and Banerjee J., eds., Geological Survey of India, Special Publication **(2000)**

40. Congalton R.G., Review of assessing the accuracy of classifications of remotely sensed data, *Remote Sens. Environ*., **37**, 35–46 **(1991)**

41. Story M. and Congalton G.R., Accuracy assessment: a user's perspective, *Photogrammetric Engineering & Remote Sensing*, **52(3)**, 397–399 **(1986)**

42. Jensen J.R., Introductory Digital Image Processing: a Remote Sensing Perspective, 2nd edition, Prentice Hall Inc., Upper Saddle River, New Jersey, USA **(1996)**

43. Congalton R.G. and Mead R.A., A quantitative method to test for consistency and correctness of photo interpretation,

Photogrammetric Engineering & Remote Sensing, **49**, 69-74 **(1983)**

44. Landis J.R. and Koch G.G., The measurement of observer agreement for categorical data, *Biometrics*, **33**, 159–174 **(1977)**

45. Kleianbum D.G., Logistic regression: A self learning text, New York, Springer, 282 **(1994)**

46. Census of India, Office of the Registrar General & Census Commissioner, India Ministry of Home Affairs, Government of India, Retrieved June 20, 2019, From http://censusindia.gov.in/2011census/dchb/1010_PART_B_DCHB_SIKKIM.pdf **(2011)**

47. BMTPC, Vulnerability Atlas of India: Earthquake, Windstorm and Flood Hazard Maps and Damaged Risk to Housing, Ministry of Housing and Urban poverty Alleviation, Government of India, First Revision **(1997)**

48. Gorsevski P.V., Jankowski P. and Gessler P.E., An heuristic approach for mapping landslide hazard by integrating fuzzy logic with analytic hierarchy process, *Control Cybern*, **35**, 121–146 **(2006)**

49. Saaty T.L., The analytical hierarchy process: planning, priority setting, resource allocation, 1st ed., RWS Publication, Pittsburgh, 502 **(1990)**

50. Muralitharan J. and Palanivel K., Groundwater targeting using remote sensing, geographical information system and analytical hierarchy process method in hard rock aquifer system, Karur district, Tamil Nadu, India, *Earth Sci. India*, **8(4)**, 827–842 **(2015)**

51. Nath S.K., Seismic hazard mapping in Sikkim Himalaya through GIS integration of site effects and strong ground motion attributes, *Natural Hazards*, **31**, 319–342 **(2004)**

52. Chauhan S., Sharma M. and Arora M.K., Landslide susceptibility zonation of the Chamoli region, Garhwal Himalayas, using logistic regression model, *Landslides*, **7**, 411–423 **(2010)**

53. Vanwalleghem T., Van Den Eeckhaut M., Poesen J., Govers G. and Deckers J., Spatial analysis of factors controlling the presence of closed depressions and gullies under forest: Application of rare event logistic regression, *Geomorphology*, **95(15)**, 504–517 **(2008)**

54. Mathew J., Jha V.K. and Rawat G.S., Landslide susceptibility zonation mapping and its validation in part of Garhwal Lesser Himalaya, India, using binary logistic regression analysis and receiver operating characteristic curve method, *Landslides*, **6**, 17-26 **(2009)**.

(Received 02nd January 2021, accepted 04th February 2021)